Influence of polymeric binder on the stability and intercalation/de-intercalation behaviour of graphite electrodes in non-aqueous solvents

R. Santhanam, M. Noel *

Central Electrochemical Research Institute, Karaikudi-630 006, India

Abstract

Cyclic voltammetric and scanning electron microscopic investigations on a highly-packed, crystalline, graphite electrode (HPC) and on a polypropylene composite graphite electrode (CPP) containing 20 wt.% polypropylene binder indicate that the latter has higher mechanical stability and higher electrochemical intercalation/de-intercalation activity. This holds for the intercalation of lithium (Li^+) and tetrabutyl ammonium (TBA^+) cations from dimethyl sulfoxide (DMSO) and dimethyl formamide (DMF), as well as for the intercalation of perchlorate (ClO_4^-) and fluoroborate (BF_4^-) anions from propylene carbonate (PC) and acetonitrile (AN). There is a linear correlation between the threshold potential for the beginning of intercalation (E_{th}) and the intercalation/de-intercalation efficiency (IDE) for cationic intercalation. In the case of anionic intercalation, two distinct linear relationships for HPC and CPP electrodes are observed. Competitive oxidation processes reduce the IDE on the HPC electrode.

1. Introduction

Graphite, one of the well-known host lattices in intercalation chemistry, exists in a wide variety of forms, purity and crystallinity [1]. Both cation and anion intercalation and de-intercalation studies have been reported on different forms of graphite materials. The graphite materials employed include: graphite foil [2], graphite sheet [3–5], graphite fibre [3,6], highly oriented pyrolytic graphite [7–9], carbon fibre [10,11], and natural graphite [11,12]. The long-term mechanical stability of many of the polycrystalline graphite electrodes is still very poor. This is one of the main challenges in the development of secondary battery systems based on graphite intercalation.

Beck and co-workers [13–15] have found that a polypropylene graphite composite electrode (CPP) containing 80 wt.% high-purity natural graphite is a good candidate for anion intercalation in strong aqueous acidic media. In the present study, the intercalation/de-intercalation behaviour of this CPP electrode is compared with a commercially available, highly-packed, crystalline, graphite material (HPC). The intercalation/de-intercalation behaviour of both cations (Li^+

and tetrabutyl ammonium ion, TBA^+) and anions [ClO_4^-, BF_4^-) in different solvents are compared. Significant differences are observed between the HPC and CPP electrodes. Attempts are also made to identify the reasons for these differences.

2. Experimental

CPP (Kropfmuhl, Normalflocke) or HPC (Graphite India) rods (3 mm diameter) embedded in Teflon were employed as working electrodes together with a platinum counter-electrode and a saturated calomel reference electrode.

The solvents and supporting electrolytes were prepared from Analar grade chemicals. The working electrode was polished thoroughly with 1/0 to 5/0 emery paper. The electrochemical activity of the electrodes was evaluated by using 2 mM ferricyanide solution ($\Delta E_p < 65$ mV) in 0.1 M potassium chloride. Cyclic voltammetric measurements were performed at 298 ± 1 K. The voltammograms were obtained with a 1 A potentiostat (Wenking, Model LB 75M, Germany), a voltage scan generator (Wenking Model VSG 72, Germany) and a x–y–t recorder (Rikadendki Model RW-201 T). Sur-

---

* Corresponding author.

Table 1
Cationic intercalation/de-intercalation parameters

Cation	Solvent	Electrode	E_{th} [a] (V)	Q_{in} (mC cm^{-2})	Q_{di} (mC cm^{-2})	Q_{di}/Q_{in} (IDE)
Li$^+$	DMSO	HPC	1.74	101.88	58.58	0.5750
	DMSO	CPP	1.70	169.68	102.52	0.6042
	DMF	HPC	1.90	66.22	25.47	0.3743
	DMF	CPP	1.94	99.05	37.07	0.3843
TBA$^+$	DMSO	HPC	1.70	60.71	40.75	0.6742
	DMSO	CPP	1.62	99.41	73.32	0.7376
	DMF	HPC	1.90	78.41	41.85	0.5337
	DMF	CPP	1.72	112.80	68.40	0.6064

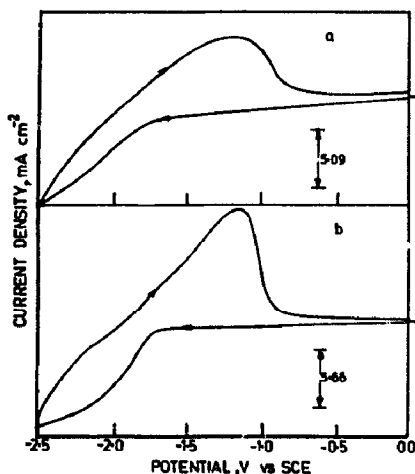[a] Threshold potential for the beginning of intercalation.

Fig. 1. Cyclic voltammograms for reductive intercalation of graphite electrodes in 0.25 M LiClO$_4$–DMSO; (a) HPC, and (b) CPP. Scan rate = 40 mV s^{-1}.

face characterization was conducted with a JEOL (Model 35CF) scanning electron microscope.

3. Results

3.1. Cationic intercalation

Cyclic voltammetric responses obtained in the present work for cationic as well as anionic intercalation were similar to those reported in the literature [2,13–15]. Typical cyclic voltammetric responses for lithium-ion intercalation in DMSO solvent on the HPC and CPP graphite materials under otherwise identical experimental conditions are shown in Fig. 1(a) and (b), respectively. Intercalation during the negative-going sweep and de-intercalation during the positive-going sweep occur in a similar potential region on both these electrodes. By contrast, significant quantitative differences exist between the voltammetric responses for HPC graphite (Fig. 1(a)) and CPP graphite (Fig. 1(b)). The intercalation charge (Q_{in}) and de-intercalation charge (Q_{di}) obtained by integrating the area under the cyclic voltammogram also differ for the two electrode materials (Table 1). The intercala-

tion/de-intercalation efficiency (IDE) is significantly higher for CPP electrode material.

Similar behaviour is exhibited by the two electrode materials for the intercalation/de-intercalation of lithium in DMF media. The threshold potential for the beginning of intercalation (E_{th}) is shifted to considerably more negative potentials in this media (Table 1). The IDE is once again higher on the CPP electrode. TBA$^+$ cations also give similar intercalation/de-intercalation responses on these two electrodes (Fig. 2). Broad intercalation/de-intercalation peaks are obtained for TBA$^+$ cation in DMSO as well as in DMF (Fig. 2(a)) for the HPC graphite electrode. The cyclic voltammetric responses are much sharper for polypropylene graphite electrodes in both DMSO and DMF (Fig. 2(b)) media. Two distinct de-intercalation peaks are also noticed before the
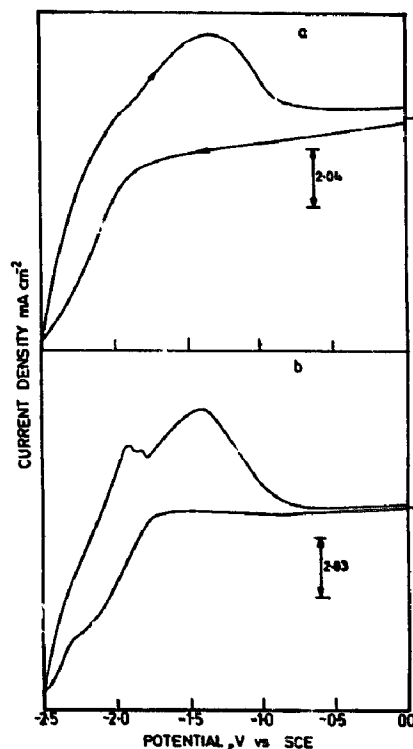

Fig. 2. Cyclic voltammograms for reductive intercalation of graphite electrodes in 0.25 M TBAP–DMF: (a) HPC, and (b) CPP. Scan rate = 40 mV s^{-1}.

Table 2
Anionic intercalation/de-intercalation parameters

Anion	Solvent	Electrode	E_{th} (V)	Q_{in} (mC cm^{-2})	Q_{di} (mC cm^{-2})	Q_{di}/Q_{in} (IDE)
ClO$_4$ $^-$	PC	HPC	1.66	152.82	76.41	0.5000
	PC	CPP	1.78	199.36	143.88	0.7217
	AN	HPC	1.68	303.16	140.09	0.4621
	AN	CPP	1.86	374.29	261.59	0.6989
BF$_4$ $^-$	PC	HPC	1.82	121.41	54.78	0.4512
	PC	CPP	1.90	332.23	236.85	0.7129
	AN	HPC	1.94	117.85	50.96	0.4324
	AN	CPP	2.00	600.95	391.70	0.6518

main de-intercalation peak for this cation in DMSO as well as in DMF solvents (Fig. 2(b)). The IDE is once again considerably higher for the CPP electrode (Table 1).

3.2. Anionic intercalation

Cyclic voltammetric measurements also confirm better IDE for CPP compared with HPC. Typical cyclic voltammetric responses of 0.25 M LiClO$_4$ in PC media in the positive potential region are shown in Fig. 3. In this medium, the E_{th} for ClO$_4$ $^-$ anion intercalation is found to be less positive for the HPC electrode than for the CPP electrode (Fig. 3 and Table 2). The de-intercalation peak, however, is much sharper for the CPP electrode (Fig. 3(b)) than for the HPC (Fig. 3(a)) electrode. Again, the IDE is higher for the CPP electrode (Table 2). Similar voltammetric responses were also obtained for these electrodes in AN media. Typical cyclic
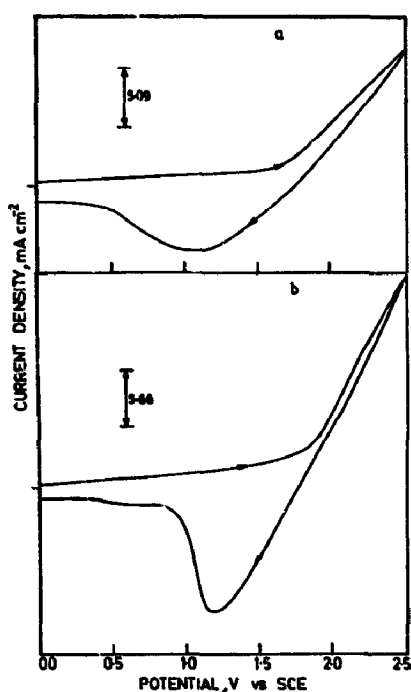

Fig. 3. Cyclic voltammograms for oxidative intercalatiion of graphite electrode in 0.25 M LiClO$_4$-PC: (a) HPC, and (b) CPP. Scan rate = 40 mV s^{-1}.
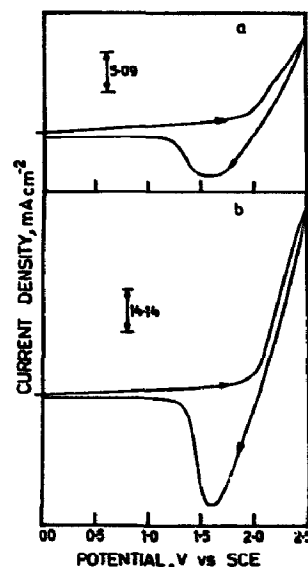

Fig. 4. Cyclic voltammograms for oxidative intercalation of graphite electrode in 0.25 M TBAFB–AN: (a) HPC, and (b) CPP. Scan rate = 40 mV s^{-1}.

voltammograms in AN for the intercalation of BF$_4$ $^-$ anions on HPC and CPP electrodes are presented in Fig. 4(a) and (b), respectively. The changes for intercalation and de-intercalation are considerably higher on the CPP electrode in both PC and AN media (Table 2). The IDE is higher on the CPP electrode.

3.3. Scanning electron microscopic studies

Scanning electron micrographs (SEMs) were recorded for HPC and CPP electrodes, both before and after intercalation and de-intercalation of lithium ions from 0.25 M LiClO$_4$ in DMSO solvent. There were no significant differences in the SEMs for freshly polished HPC and CPP electrodes. Both the electrodes were subjected to cationic intercalation at − 2.5 V and anionic intercalation at + 2.5 V for 7 min under identical experimental conditions so that the surface transformations could be directly compared. The intercalated samples were subsequently de-intercalated at − 1.4 V for cationic and + 1.4 V for anionic systems, again for a period of 7 min. The SEMs recorded after this treatment are presented in Figs. 5 and 6, respectively.
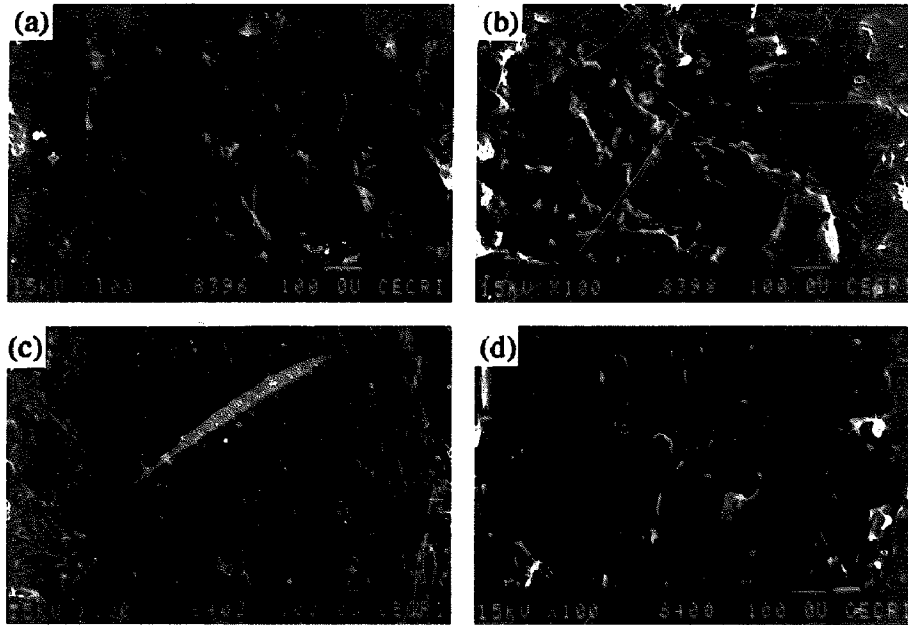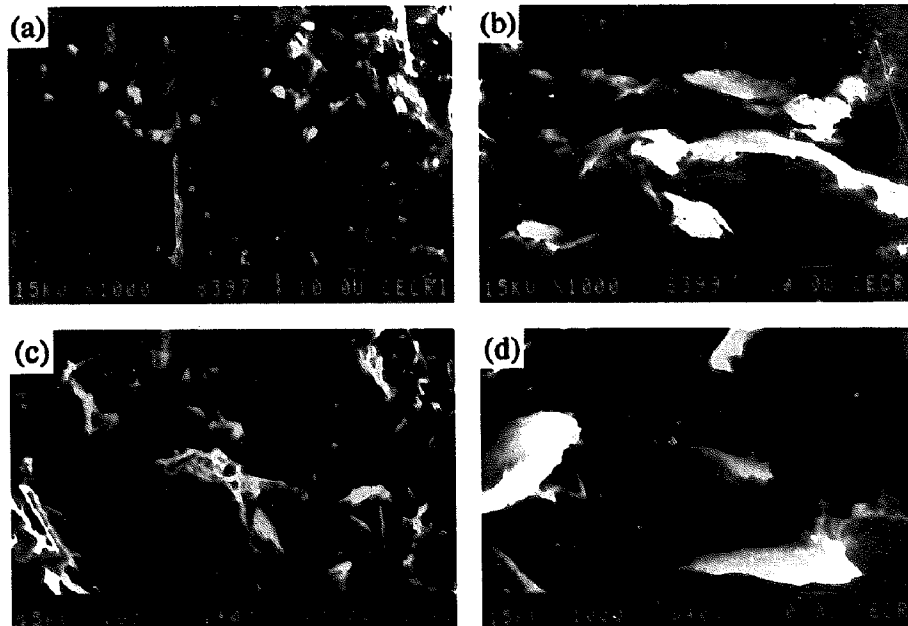
Fig. 5. Scanning electron micrographs of graphite electrodes obtained from 0.25 M LiClO₄ solution. Intercalation and de-intercalation for 7 min at − 2.5 and − 1.4 V, respectively. Intercalated graphite: (a) HPC, ×100, and (b) CPP, ×100. De-intercalated graphite: (c) HPC, ×100, and (d) CPP, ×100.

Fig. 6. Scanning electron micrographs of graphite electrodes obtained from 0.25 M LiClO₄ solution. Intercalation and de-intercalation for 7 min at − 2.5 and − 1.4 V, respectively. Intercalated graphite: (a) HPC, ×1000, and (b) CPP×1000. De-intercalated graphite: (c) HPC×1000, and (d) CPP×1000.

Both HPC and CPP electrodes undergo some surface roughening during the intercalation of lithium ions, as evidenced in Fig. 5(a) and (b), respectively. The surface of intercalated HPC exhibits a considerably higher microroughness (Fig. 5(a)) compared with that of CPP under identical conditions (Fig. 5(b)). This feature becomes even more apparent after intercalation and subsequent de-intercalation (see Fig. 5(c) and (d)). The HPC electrode surface clearly develops a very rough surface with numerous small

particles in addition to fairly large pits (Fig. 5(c)). The graphite plates embedded in polypropylene are not roughened to any significant extent, either during polishing or during intercalation/de-intercalation. Hence, the density of smaller particles is considerably lower on CPP (Fig. 5(d)). Sharp lines corresponding to graphite plates with edge orientation towards the surface are also evident (Fig. 5(d)).

The difference between HPC and CPP electrodes becomes even more obvious at higher magnification. The density of

graphite particles after intercalation on HPC (Fig. 6(a)) and CPP (Fig. 6(b)) can be directly compared. The CPP surface contains only a few large graphite plates (Fig. 6(b)). By contrast, the presence of a very high concentration of graphite particles with widely varying particle sizes is clearly observed on an intercalated HPC surface (Fig. 6(a)). The SEMs of CPP electrodes before and after de-intercalation are similar, as demonstrated by Fig. 6(b) and (d), respectively. The roughness does not increase significantly. On the other hand, the roughness of the HPC electrode even, after a single intercalation/de-intercalation cycle, is greatly increased (Fig. 6(c)). The smaller graphite particles probably peel off from the electrode surface very quickly. Nevertheless, regions of the de-intercalated HPC surface still contain smaller particles (see top right hand corner of Fig. 6(c)).

4. Discussion

The SEM studies clearly establish the advantages of using a CPP electrode for intercalation/de-intercalation, as opposed to a HPC electrode. The polypropylene regions hold quite strongly the graphite plates of different orientations. Hence, they do not undergo roughening during the polishing operation. Moreover, since polypropylene is not soluble in the solvent-supporting electrolyte system, the embedded graphite particles are strongly held during both intercalation and de-intercalation. By contrast, the graphite plates undergo exfoliation during both intercalation and de-intercalation. This probably accounts for the similarity in the electron microscopic responses for the intercalated as well as the de-intercalated CPP samples (compare Fig. 5(b) and (d) with Fig. 6(b) and (d)). Apart from these mechanical advantages of using CPP, cyclic voltammetric studies also indicate some electrochemically advantageous features. The cyclic voltammetric results presented above consistently show that the CPP electrode is a better material of choice for the intercalation/de-intercalation process when compared with the HPC electrode. The responses can be quantitatively compared at two different levels. First, the individual intercalation and de-intercalation charges can be compared. Second, the overall IDEs can be compared.

The geometric surface area of the HPC and CPP electrodes employed in the present study are the same. The CPP electrode is, however, a composite material that contains 20 wt.% polypropylene and 80 wt.% natural graphite. Hence, lower intercalation charges are expected on the CPP electrode. For the eight systems chosen for comparison in this work, the Q_{in} for the CPP electrodes is almost equal or considerably higher than that for the HPC electrode (Tables 1 and 2). The maximum difference (over $\sim 100\%$) in the Q_{in} value for CPP is noticed in the case of fluoroborate anion in acetonitrile media.

The enhanced Q_{in} values observed in most of the cases for the CPP electrode may probably be associated with the crystal size of the graphite material involved. The HPC material may actually contain graphite crystallites with relatively smaller
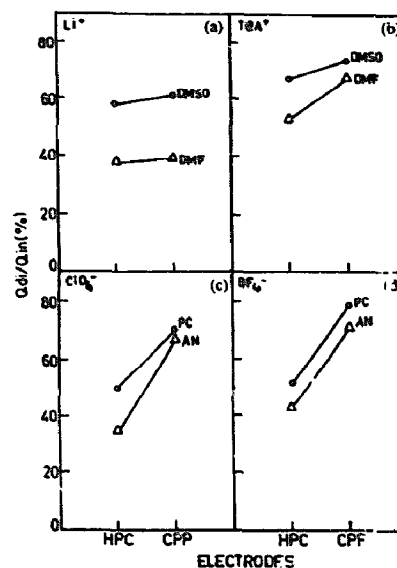

Fig. 7. Plots of relationship between charge recovery ratio and electrode material (HPC and CPP). Concentration of salt = 0.15 M. Scan rate = 40 mV s⁻¹.

sizes. During the polishing operation, small carbon powders are found to become embedded on the electrode surface. With smaller particle sizes, the true electrode surface area may actually be increased. The penetration depth of the ionic species would be much higher, however, if crystallites of larger dimension are employed. The polypropylene film may also help in retaining the graphite crystal size at the surface during the polishing operation.

The IDE is always higher on the CPP electrode. The relative improvements depend, however, on the nature of the solvent-supporting electrolyte systems. This aspect is quantitatively brought out in Fig. 7 — there is very little improvement in the IDE in the case of Li^+ ions (Fig. 7(a)). The improvement is slightly better in the case of TBA^+ cations (Fig. 7(b)). For anions, the improvement in IDE is very significant for the CPP electrode (Fig. 7(c) and (d)).

To understand the influence of the nature of the polymeric material on the performance of graphite electrodes, attempts were made to determine some correlation between the cyclic voltammetric parameters in different solvents (Tables 1 and 2) and the over all IDE. The E_{th} is found to give an interesting correlation with the IDE. In the case of cationic intercalation, a linear relationship between E_{th} and IDE is found to exist (Fig. 8(b)). It is noteworthy that this relationship holds for both of the electrodes in either DMSO or DMF media for Li^+ and TBA^+ cations. Lower E_{th} values always correspond with higher IDE values. Such a relationship is possible only if all the intercalation and de-intercalation processes compete with the same competitive electrochemical process. In this case, it appears that hydrogen evolution from the trace level of water present in the solvent-supporting electrolyte systems, rather than the decomposition of solvent-supporting electrolyte itself, is the competitive electrochemical process.
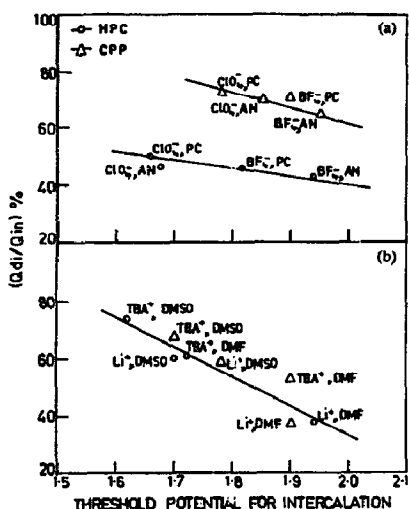
Fig. 8. Plots of relationship between charge recovery ratio and threshold potential for intercalation at two different electrodes in different solvents: (a) anions, and (b) cations. Scan rate = 40 mV s^{-1}.

Another interesting observation is noticed in the case of anionic intercalation. Here, individual correlation between E_{th} and IDE does exist for the HPC and the CPP electrodes (Fig. 8(a)). The CPP electrodes exhibit a higher E_{th} for intercalation, and also yield a higher IDE. In this case, it appears that for a HPC electrode, the E_{th} actually corresponds to simultaneous oxygen evolution and anion intercalation. Hence, the apparently higher E_{th} for the CPP electrode is actually due to the suppression of oxygen evolution. The polymeric binder in the CPP electrode imparts some hydrophobicity to the graphite material and, hence, graphite oxidation, formation of graphite oxide layers and oxygen evolution are suppressed on this electrode material.

5. Conclusions

The present investigation was undertaken with the main objective of determining whether polypropylene composite graphite material imparts greater mechanical strength. Some loss in electrochemical activity was indeed anticipated due to the presence of an insulating polymer layer. Quite surprisingly. it is observed that the polypropylene layer, in addition to improving the mechanical stability of the graphite elec-

trode, also leads to higher intercalation charge and higher IDE. The competitive process for cationic intercalation (probably hydrogen evolution) does not depend on the electrode material. The competitive anodic processes namely, graphite surface oxidation and oxygen evolution, occur at much lower potentials on HPC graphite material than on relatively hydrophobic CPP graphite material. Hence, the difference in IDE is much higher between the two electrodes for anion intercalation.

From a practical stand point, it is certainly better to employ a CPP electrode for a more detailed investigation of cationic and anionic intercalation in different solvents.

References

[1] K. Kinoshita, Carbon, Electrochemical and Physicochemical Properties, Wiley, New York, 1988.
[2] J.O. Besenhard and H.P. Fritz, J. Electroanal. Chem., 53 (1974) 329.
[3] Y. Matsuda, M. Morita and H. Katsuma, Denki Kagaku, 51 (1983) 744.
[4] Y. Maeda, Bull. Chem. Soc. Jpn., 62 (1989) 3711.
[5] Y. Maeda, J. Electrochem. Soc., 137 (1990) 3047.
[6] T. Ohzuku, Z. Takehara and S. Yoshizawa, Denki Kagaku, 46 (1978) 438.
[7] B. Marcus and Ph. Touzain, Synth. Met., 23 (1988) 13.
[8] D. Billaud, F.X. Henry and P. Willmann, Mater. Res. Bull., 28 (1993) 477.
[9] T. Tran and K. Kinoshita, J. Electroanal. Chem., 386 (1995) 221.
[10] Y. Maeda and S. Harada, Synth. Met., 31 (1989) 389.
[11] R. Yazami, K. Zaghib and M. Deschamps, J. Power Sources, 52 (1994) 55.
[12] J. Simonet, J. Electroanal. Chem., 75 (1977) 719.
[13] F. Beck, H. Junge and H. Krohn, J. Appl. Electrochem., 26 (1981) 799.
[14] F. Beck, H. Krohn and W. Kaiser, J. Appl. Electrochem., 12 (1982) 505.
[15] F. Beck and H. Krohn, Synth. Met., 14 (1986) 137.